Asian Journal of Chemistry; Vol. 33, No. 12 (2021), 3089-3098

ASIAN JOURNAL OF CHEMISTRY

https://doi.org/10.14233/ajchem.2021.23438

Computational Exploration of 1-Amidino-O-(*n*-butyl) Urea (AB^{n}UH) with Natural Atomic Orbitals, Natural Bond Orbital, Vibrational Analysis and Simulated UV-Visible Spectra

NAOREM SHUBHASCHANDRA SINGH[1,*] and SAGOLSEM MANIMUKTA DEVI[2]

[1]Department of Chemistry, D.M. College of Science Imphal, Dhanamanjuri University, Manipur-795001, India
[2]Department of Chemistry, Naorem Birahari College, Khundrakpam, Imphal East District-795114, India

*Corresponding author: E-mail: shubhasnaorem@yahoo.com

Received: 30 July 2021; *Accepted*: 8 October 2021; *Published online*: 6 December 2021; AJC-20603

Theoretical treatment of 1-amidino-O-(*n*-butyl)urea (AB^{n}UH) have been performed by DFT/B3LYP with 6-311++ G (d,p) basis set using Gaussian 09W. The compound has been analyzed on the basis of electronic structure, hybridization of the atoms, charge delocalization, hyper-conjugative interactions, vibrational modes, *etc.* NBO analysis was performed to figure out any charge transfer among the localized bond and lone pair of the proposed compound.

Keywords: Alkyl ureas, Natural atomic orbital, Natural bond orbital, Hyper-conjugative interaction, Frontier orbitals, DFT.

INTRODUCTION

1-Amidino-O-alkylureas are considered to be the powerful coordinating ligands [1] and were synthesized while attempting for a biguanide derivative. Despite of many attempts on syntheses since 1961 it is also extended to exploit further the transition metal complexes when coordinated with 1-amidino-O-alkyl-ureas. Among the 1-amidino-(alkyl)ureas, the 1-amidino-O-(*n*-butyl)urea (AB^{n}UH) has been found to use in synthesizing Cu(II), Ni(II), Co(II), Co(III) complexes [2-4]. Till date, it is found from literature survey that no theoretical calculations regarding molecular orbital energies, the electronic properties, the natural bonding orbitals analysis and vibrational modes of the compound have not been conducted. Therefore, we report herein the theoretical exploration of the compound through density functional theory (DFT) for which it is known for its reliability in reproducing experimental data [5] aiming at describing and characterizing the molecular structure, predicting molecular frontier energy (HOMO and LUMO orbitals), electronegativity (χ), hardness (η), softness (S), molecular electrostatic potential maps (MEP), Mulliken charge, the natural bonding orbital analysis and harmonic vibrational properties of the proposed compound. Chemical reactivity and stability of the compound [6] has been derived from the HOMO and LUMO energies, which are considered helpful in designing new drug when incorporated with maximum absorption. Lower energy gap between the energies defines higher reactivity due to easy electron excitation from the ground to the higher states that would lead to best bonding of the molecule. The molecule having such a small gap of energies are referred to as soft molecules while having high polarizability and with large gap referred to as hard molecule. These energy values are also useful in determining transfer of charge, intramolecular interaction, molecular transport properties and chemical reactivity descriptors like hardness, chemical potential, electronegativity and electrophilicity index [7,8]. As a convincing tool for the elucidation of residual resonance delocalization effects of molecule, NBO analysis illustrates by deciphering molecular wave function in terms of Lewis structures, charge, bond order, bond type, hybridization, resonance, donor-acceptor interaction, *etc.* [9].

COMPUTATIONAL METHODS

Theoretical calculation was performed with DFT/B3LYP method in the 6-311++G(d,p) level using Gaussian 09W to study electron population in subshells of atomic orbitals, charge delocalization, electron densities of atoms, molecular orbitals as well as harmonic vibration properties. The same level of calculation was also used with TD-DFT/B3LYP to study electron

transition, absorption wavelength, excitation energies and solvent effect on the simulated UV-visible spectra. The calculated potential energy distribution (PED) was performed for a detailed vibrational assignments using VEDA program 4.0. Population analysis for the natural bond orbitals (NBO) was calculated using NBO program 3.1 equipped with Gaussian 09W.

RESULTS AND DISCUSSION

The optimized structure of 1-amidino-O-(*n*-butyl) urea (AB^nUH) predicted by DFT/B3LYP method using 6-311++G (d,p) basis set is shown in Fig. 1.

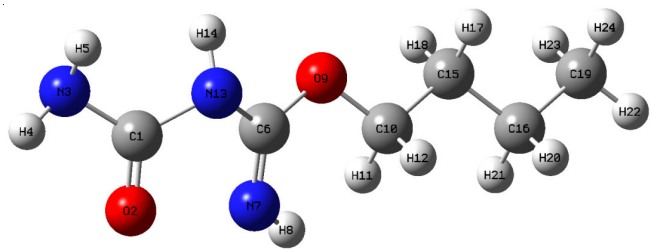

Fig. 1. Optimized structure of 1-amidino-O-(-*n*-butyl) urea by B3LYP/6-311++G(d,p) method

The Mulliken atomic charges of the optimized structure of the compound are calculated and tabulated in Table-1. The optimized structure of the compound is used to study, molecular polarizability, electronic structure and a number of properties of molecular systems [10] and donor-acceptor pairs involving the charge transfer in the molecule [11,12]. It is worthy to mention that H4, H5, H8, H11, H12, H14, H17, H18, H20, H21, H22, H23, H24, C6 of the molecule possess positive charges while N3, C1, O2, N13, N7, O9, C10, C15, C16 and C19 atoms possess negative charges. The results are given in Table-1b. The magnitude of the carbon atomic charges found to be either positive or negative between 0.183 to -0.533 with maximum value in the methyl group. Maximum positive atomic charge of about 0.278 is obtained for H4 in NH_2 group. The presence of large negative charge on C and large positive charge on H suggested the formation of no intermolecular interaction. The corresponding Mullliken's plot is shown in Fig. 2.

Frontier molecular orbitals (FMOs): Frontier molecular orbitals (FMOs) *i.e.* the HOMOs and the LUMOs are important parameters for quantum chemistry and UV-visible spectral studies

TABLE-1a
BOND LENGTH CALCULATED BY B3LYP/6-311G++(d,p)

Bond	Bond length (nm)	Bond	Bond length (nm)
C1-N13	1.470	C10-H12	1.070
C1-O2	1.258	C15-C10	1.540
C1-N3	1.470	C15-H18	1.070
N3-H4	1.00	C15-H17	1.070
N3-H5	1.00	C15-C16	1.540
N13-H14	1.00	C16-H21	1.070
N13-C6	1.470	C16-H20	1.070
N7-H8	1.00	C16-C19	1.540
C6-N7	1.294	C19-H22	1.070
O9-C6	1.430	C19-H24	1.070
O9-C10	1.430	C19-H23	1.070
C10-H11	1.070		

TABLE-1b
MULLIKEN ATOMIC CHARGE
CALCULATED BY B3LYP/6-311G++(d,p)

Atom	Mulliken charge	Atom	Mulliken charge
C1	-0.057	N13	-0.129
O2	-0.202	H14	0.260
N3	-0.280	C15	-0.279
H4	0.278	C16	-0.167
H5	0.216	H17	0.151
C6	0.183	H18	0.147
N7	-0.266	C19	-0.533
H8	0.218	H20	0.125
O9	-0.079	H21	0.124
C10	-0.464	H22	0.138
H11	0.142	H23	0.132
H12	0.213	H24	0.131

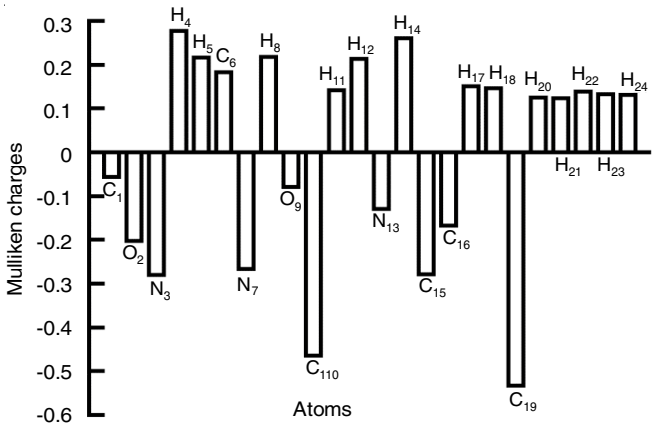

Fig. 2. Charge distribution analysis for 1-amidino-O-(*n*-butyl) urea (AB^nUH)

[13]. They are used to understand how a molecule interacts with other during chemical reaction. HOMOs are electron donor for the outermost orbital while LUMO accepts innermost free electron orbital [14]. The Frontier orbital gap determines the chemical reactivity and kinetic stability of the compound [13]. A compound with a small frontier orbital gap is generally associated with a high chemical reactivity, low kinetic stability and is also termed as soft molecule [15]. The HOMO and LUMO along with the surface of the compound in the gaseous state are shown in Fig. 3. The calculated energy values for the compound in gaseous state are given as E_{HOMO} = –0.22346 au, E_{LUMO} = –0.02373 au and $\Delta E_{LUMO-HOMO}$ = 0.19973 au. The calculation indicates that the titled compound have 333 MOs of which 43 orbitals are occupied molecular orbitals. The descriptors that are useful to analyze the global reactivity of the compound such as electronegativity, hardness, softness and electrophilicity index are calculated [13] using ionization potential ($I = -E_{HOMO}$) and electron affinity ($A = -E_{LUMO}$). The absolute electronegativity $\left(\chi = \frac{I+A}{2}\right)$, chemical hardness $\left(\eta = \frac{I-A}{2}\right)$, chemical softness $\left(S = \frac{1}{2\eta}\right)$, electrophilicity index $\left(\omega = \frac{\mu^2}{2\eta}; \mu = -\frac{I+A}{2}\right)$ were calculated and presented in Table-2.

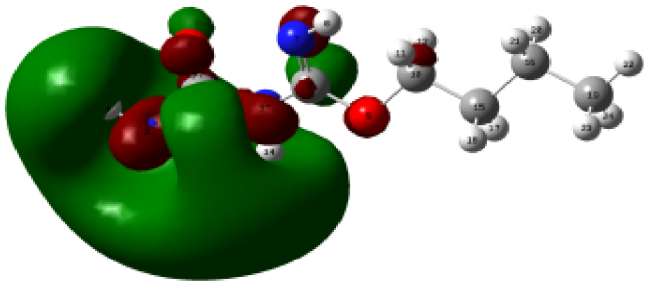

E_{LUMO} = -0.02373 au

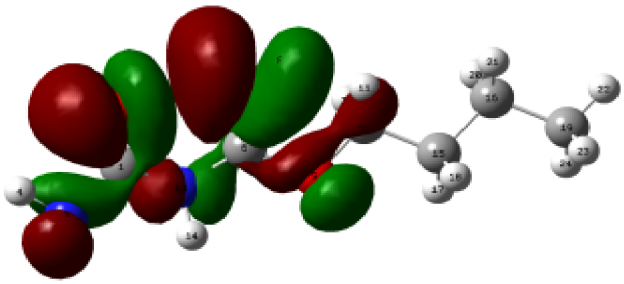

E_{HOMO} = -0.22346 au

Fig. 3. Molecular orbital surfaces and energies of HOMO and LUMO

From Fig. 3, it is observed that HOMO orbital is located mainly in the urea group due to the presence of N and O containing functional group and extended upto the carbon atom (C10) of butyl group while LUMO orbital is concentrated mainly on amide end of the compound due to accumulation of negatively charge atoms. It has been reported that organic molecules are classified as marginal electrophile with $\omega < 0.8$ eV, moderate electrophile with $0.8 < \omega < 1.5$ eV and strong electrophile having $\omega > 1.5$ eV [16]. Since, the compound AB^{n}UH has $\omega =$ 2.081179 eV also indicates a strong electrophile.

Analysis of molecular electrostatic potential (MEP) surface: The molecular electrostatic potential (MEP) surface of a compound is a plot for different electrostatics potential value represented by different colour. The red colour in the plot indicates maximum negative region at which electrophilic attack is preferred and the blue colour indicates the preferred site for nucleophilic attack. The MEP plot of the AB^{n}UH is shown in Fig. 4. The plot suggested that the electronegative potential region is between C1O2 and N7H8 groups with electrostatic surface map value about -0.765313 and the electropositive region is found around N3H5 and N13H14 groups with electrostatic surface map value of about 0.0544429. The rest of the compound appears to show neutral electrostatic potential.

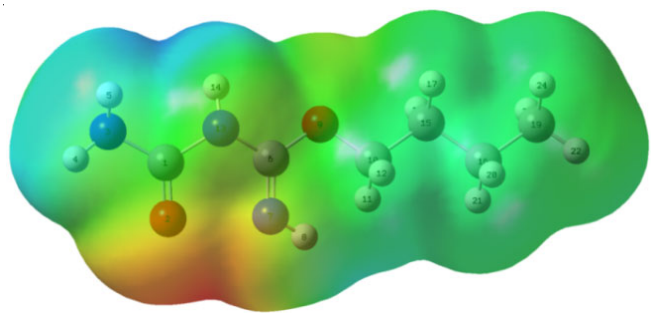

Fig. 4. Electrostatic potential surface of 1-amidino-O-(*n*-butyl) urea (AB^{n}UH)

Natural atomic orbitals (NAO): The occupancies along with energies of bonding molecular orbitals of the molecules AB^{n}UH are calculated at B3LYP/6-311++(d,p) level of theory and are presented in Table-3, which gives the evidence for the delocalization of charge, bond lengths, *etc.* as shown in the optimized structure of the molecule (Fig. 1).

Natural population analysis: The analysis [17] described the distribution of electrons in various subshells of their atomic orbitals of the molecule AB^{n}UH. The accumulation of charges on the individual atom and accumulation of electrons in the core, valence and Rydberg subshells are presented in Table-4. The molecule AB^{n}UH has most electronegative charge of -0.82353e accumulated in N3 followed by N13 with -0.67722e and N7 with -0.67493e. The oxygen O9 and O2 has also observed to accumulate with -0.58851e and with -0.56363e, respectively. The distributions of charges, where the electronegative atoms have the tendency to donate electron while the electropositive atom such as C1 (with 0.79583e) and C6 (with 0.71302e) have tendency to accept an electron, also support the electrostatic surface plot as given in Fig. 4.

Further the natural population analysis has shown that 86 electrons of the molecule are distributed in the sub-shells as follows:

	Natural population
Core	21.99349 (99.9704% of 22)
Valence	63.75298 (99.6140% of 64)
Natural minimal basis	85.74647 (99.7052% of 86)
Natural Rydberg basis	0.25353 (0.2948% of 86)

TABLE-2
CALCULATED FRONTIER ORBITAL ENERGIES AND GLOBAL DESCRIPTORS OF
1-AMIDINO-O-(*n*-BUTYL) UREA (AB^{n}UH) USING DFT/B3LYP WITH 6-311++G(d,p) LEVEL

Parameters	Molecule in			
	Gaseous state	Water	Methanol	Ethanol
E_{HOMO} (au)	-0.22346	-0.01128	-0.01153	-0.01166
E_{LUMO} (au)	-0.02373	-0.27249	-0.27218	-0.27201
E_{LUMO}–E_{HOMO} (au)	0.19973	-0.26121	-0.26065	-0.26035
Ionization potential (I, a.u.)	0.22346	0.01128	0.01153	0.0116
Electron affinity (A, a.u.)	0.02373	0.27249	0.27218	0.27201
Electronegativity (χ, a.u.)	0.123595	0.14188	0.14186	0.14183
Chemical hardness (η, a.u.)	0.099865	-0.13061	0.13033	-0.13018
Chemical softness (S, a.u.)	5.006759	-3.82834	3.83656	-3.84098
Electrophilicity index (ω, a.u.)	0.076482 (2.081179 eV)	-0.07707 (-2.09717 eV)	-0.54424 (-2.10079 eV)	-0.07727 (-2.10262 eV)

TABLE-3
OCCUPANCIES AND ENERGIES OF BONDING MOLECULAR ORBITALS OF 1AMIDINO-O-(*n*-BUTYL) UREA (AB^{n}UH)

Atomic orbitals	Occupancy (e)	Energy (a.u.)
BD(1) C1-O2	1.99539	-1.00273
BD(2) C1-O2	1.99083	-0.36375
BD(1) C1-N3	1.99276	-0.76863
BD(1) C1-N13	1.98146	-0.76912
BD(1) N3-H4	1.98434	-0.67084
BD(1) N3-H5	1.98385	-0.66751
BD(1) C6-N7	1.99420	-0.88899
BD(2) C6-N7	1.98553	-0.33253
BD(1) C6-O9	1.98928	-0.83669
BD(1) C6-N13	1.97876	-0.77217
BD(1) N7-H8	1.96628	-0.62588
BD(1) O9-C10	1.98385	-0.82906
BD(1) C10-H11	1.98653	-0.53957
BD(1) C10-H12	1.98806	-0.53424
BD(1) C10-C15	1.98158	-0.60857
BD(1) N13-H14	1.97224	-0.66826
BD(1) C15-C16	1.97848	-0.59375
BD(1) C15-H17	1.98137	-0.50863
BD(1) C15-H18	1.98148	-0.50866
BD(1) C16-C19	1.98729	-0.59237
BD(1) C16-H20	1.98253	-0.50739
BD(1) C16-H21	1.98253	-0.50749
BD(1) C19-H22	1.98996	-0.50870
BD(1) C19-H23	1.99055	-0.51066
BD(1) C19-H24	1.99053	-0.51071

TABLE-4
ACCUMULATION OF NATURAL CHARGES, POPULATION OF ELECTRONS IN CORE, VALENCE, RYDBERG ORBITALS OF AB^{n}UH

Atoms	Charge	Natural population (e)			Total (e)
		Core	Valence	Rydberg	
C1	0.79583	1.99963	3.15977	0.04477	5.20417
O2	-0.56363	1.99977	6.55083	0.01303	8.56363
N3	-0.82353	1.99945	5.80724	0.01684	7.82353
H4	0.38972	0.00000	0.60662	0.00367	0.61028
H5	0.35839	0.00000	0.63792	0.00368	0.64161
C6	0.71302	1.99927	3.25023	0.03748	5.28698
N7	-0.67493	1.99936	5.65942	0.01615	7.67493
H8	0.34742	0.00000	0.64905	0.00353	0.65258
O9	-0.58851	1.99974	6.57086	0.01791	8.58851
C10	-0.00959	1.99909	3.98892	0.02159	6.00959
H11	0.15201	0.00000	0.84432	0.00367	0.84799
H12	0.17131	0.00000	0.82589	0.00280	0.82869
N13	-0.67722	1.99932	5.65955	0.01835	7.67722
H14	0.38475	0.00000	0.61193	0.00332	0.61525
C15	-0.38106	1.99925	4.36840	0.01340	6.38106
C16	-0.37101	1.99928	4.36111	0.01063	6.37101
H17	0.19396	0.00000	0.80372	0.00231	0.80604
H18	0.19443	0.00000	0.80328	0.00229	0.80557
C19	-0.55923	1.99933	4.55195	0.00796	6.55923
H20	0.18485	0.00000	0.81272	0.00243	0.81515
H21	0.18429	0.00000	0.81321	0.00250	0.81571
H22	0.19664	0.00000	0.80175	0.00160	0.80336
H23	0.19113	0.00000	0.80706	0.00181	0.80887
H24	0.19096	0.00000	0.80722	0.00182	0.80904
Total	0.00000	21.99349	63.75298	0.25353	86.00000

Natural bond orbitals analysis (NBO): NBO analysis explains the strong hyper conjugative forces or interactions of π-electrons and electronic density redistribution in bonding and antibonding orbitals [18] of AB^{n}UH molecule with the help of second-order perturbation theory (Table-5). The second-order perturbation theory determined the most accurate possible delocalized type of interaction based on electron donor orbitals (filled or Lewis type NBOs) and acceptor orbitals (empty or non-Lewis type NBOs) [19]. When the interaction between electron donors and electron acceptors is intense there is greater extent of conjugation in the whole molecular system with larger stabilization energy. Some electron donor orbital, acceptor orbital and the interacting stabilizing energy resulting from the second order micro-disturbance theory are reported [20,21]. Larger stabilization energy is shown due to greater extent of conjugation of the molecular system when there is strong interaction between donor and acceptors The analysis stresses the role of intra and intermolecular orbital interaction in the compound, particularly charge transfer or conjugative interaction [22]. DFT/B3LYP/6-3116++ G(d,p) level was used to perform NBO analysis. The stabilization energy $E^{(2)}$ was estimated between donor NBO (i) and acceptor NBO (j) as:

$$E^2 = q_i \frac{(F_{i,j})^2}{\varepsilon_j - \varepsilon_i} \quad (1)$$

where q_i is the orbital occupancy, ε_i, ε_j are diagonal element and $F_{i,j}$ is the off-diagonal NBO Fock matrix element [18].

Table-5 listed the hyperconjugative interaction of lp(2) O2 orbital and σ*(C1-N13) giving stabilizing energy of 24.72 kcal/mol, lp(1)N3 orbital and π*(C1-O2) with 23.89 kcal/mol, lp(2)O2 orbital and σ*(C1-N3) with 22.12 kcal/mol, lp(1)N13 orbital and π*(C1-O2) with 21.32 kcal/mol, lp(2)O9 orbital and π*(C6-N7) with 21.19 kcal/mol which are considerably significant for the stabilization of the present molecular system. The interaction energy related to resonance of the molecule is shown by lp(2)O2 → σ*C1-N13 with 24.72 kcal/mol and lp(2)O2 → σ*C1 –N3 with 22.12 kcal/mol. In a similar manner the lone pair interaction with antibonding bonds are shown by the lp(2)O9 → σ*C6–N7 with 21.19 kcal/mol energy, lp(2)O9 → σ*C10–H12 with 5.73 kcal/mol, lp(2)O9 → σ*C10–H11 with 4.75 kcal/mol, lp(2)O9 → σ*C6–N7 with 1.41 kcal/mol and lp(2)O9 → σ*C6–N13 with 2.17 kcal/mol order of stabilizing energy of the molecular system. The interaction between πC–C orbitals and antibonding πC–C orbitals has little contribution towards the stabilization of the molecular system.

The calculated occupancies of natural orbitals along with their natural hybrids on atoms consisting Lewis type (σ and π or lone pair) orbitals, the non-Lewis (acceptor or unfilled) orbitals and Rydberg orbitals originating orbitals outside the atomic valence shell are given in Table-6. It is observed that the bond σC1-O2 bond is formed from $sp^{1.91}$ hybrid on C, which is a mixture of 34.28% of s, 65.56% of p and 0.16% of d orbitals). On the other hand, σN3-H5 is formed from a $sp^{3.19}$ (N3) hybrid on nitrogen (which is the mixture of 23.87% s, 76.04% p and 0.08% d orbitals. The oxygen lone pair atoms, O2 of (AB^{n}UH) showed that the atom contributes to both *s*-type and *p*-type subshells while the other remaining hybrid atomic orbital of lone pair O9 and all bonding and

TABLE-5
SECOND-ORDER THEORY ANALYSIS OF FOCK-MATRIX ON NBO BASIS FOR 1-AMIDINO-O-(*n*-BUTYL)UREA (AB^{n}UH)

Donor (i)	Type	ED (i)	Acceptor (j)	Type	ED (j)	E_2 (kcal/mol)	E(j)-E(i) (a.u.)	F(i,j) (a.u.)
O2	LP(2)	1.84627	C1-N13	σ*	0.08624	24.72	0.54	0.105
N3	LP(1)	1.86013	C1-O2	π*	0.26091	23.89	0.35	0.084
O2	LP(2)	1.84627	C1-N3	σ*	0.06931	22.12	0.54	0.100
N13	LP(1)	1.79377	C1-O2	π*	0.26091	21.32	0.36	0.079
O9	LP(2)	1.86596	C6-N7	π*	0.19767	21.19	0.34	0.077
N7	LP(1)	1.89597	C6-O9	σ*	0.08883	18.18	0.60	0.094
N13	LP(1)	1.79377	C6-N7	π*	0.19767	16.93	0.38	0.072
O2	LP(1)	1.97900	C1	Ry*	0.01544	15.06	1.55	0.137
N7-H8	σ	1.96628	C6-N13	σ*	0.05443	8.04	0.93	0.077
N7	LP(1)	1.89597	C6	Ry*	0.01543	6.65	1.21	0.082
O9	LP(2)	1.86596	C10-H12	σ*	0.02177	5.73	0.75	0.060
O9	LP(2)	1.86596	C10-H11	σ*	0.02730	4.75	0.74	0.054
O9	LP(1)	1.96740	C6-N7	σ*	0.02022	4.74	1.17	0.067
N3-H4	σ	1.98434	C1-N13	σ*	0.08624	4.10	0.97	0.057
N3-H5	σ	1.98385	C1-O2	σ*	0.01366	3.88	1.19	0.061
N7	LP(1)	1.89597	C6-N13	σ*	0.05443	3.82	0.64	0.045
C1-N13	σ	1.98146	C6-O9	σ*	0.08883	3.61	1.03	0.055
O9-C10	σ	1.98385	C6-N13	σ*	0.05443	3.61	1.13	0.058
N13-H14	σ	1.97224	C1-O2	σ*	0.01366	3.15	1.19	0.055
O9	LP(1)	1.96740	C6	Ry*	0.01543	2.97	1.46	0.059
N7-H8	σ	1.96628	C6	Ry*	0.01543	2.96	1.49	0.060
N13-H14	σ	1.97224	C6-N7	σ*	0.02022	2.94	1.25	0.054
C15-C16	σ	1.97848	O9-C10	σ*	0.02071	2.81	0.87	0.044
C6-N13	σ	1.97876	C1-N3	σ*	0.06931	2.79	1.07	0.049
O2	LP(1)	1.97900	C1	Ry*	0.01039	2.77	1.52	0.060
C6-N13	σ	1.97876	N7-H8	σ*	0.01276	2.64	1.26	0.052
C16-H20	σ	1.98253	C15-H18	σ*	0.01410	2.42	0.94	0.043
C16-H21	σ	1.98253	C15-H17	σ*	0.01430	2.42	0.94	0.043
C19-H22	σ	1.98996	C15-C16	σ*	0.01083	2.42	0.89	0.041
C15-H17	σ	1.98137	C16-H21	σ*	0.01455	2.39	0.94	0.042
C15-H18	σ	1.98148	C16-H20	σ*	0.01453	2.38	0.94	0.042
C19-H23	σ	1.99055	C16-H20	σ*	0.01453	2.38	0.94	0.042
C19-H24	σ	1.99053	C16-H21	σ*	0.01455	2.38	0.94	0.042
C10-C15	σ	1.98158	C6-O9	σ*	0.08883	2.36	0.87	0.041
C10-H12	σ	1.98806	C15-H18	σ*	0.01410	2.29	0.97	0.042
C16-H21	σ	1.98253	C19-H24	σ*	0.00744	2.22	0.94	0.041
C16-H20	σ	1.98253	C19-H23	σ*	0.00744	2.21	0.94	0.041
C10-H11	σ	1.98653	C15-H17	σ*	0.01430	2.20	0.97	0.041
O9	LP(2)	1.86596	C6-N13	σ*	0.05443	2.17	0.63	0.034
C15-H17	σ	1.98137	C10-H11	σ*	0.02730	2.15	0.92	0.040
C15-H18	σ	1.98148	C10-H12	σ*	0.02177	2.12	0.92	0.039
C16-C19	σ	1.98729	C10-C15	σ*	0.01628	1.94	0.96	0.039
O9	LP(1)	1.96740	C10	Ry*	0.00417	1.92	1.69	0.051
C10-C15	σ	1.98158	C16-C19	σ*	0.00613	1.83	0.98	0.038
O2	LP(1)	1.97900	C1-N3	σ*	0.06931	1.58	1.01	0.036
N13-H14	σ	1.97224	C6-N7	π*	0.19767	1.51	0.68	0.030
O2	LP(1)	1.97900	C1-N13	σ*	0.08624	1.47	1.00	0.035
N7-H8	σ	1.96628	C6-O9	σ*	0.08883	1.42	0.88	0.032
N3	LP(1)	1.86013	H5	Ry*	0.00109	1.42	1.95	0.049
C1-O2	σ	1.99539	C1	Ry*	0.01544	1.41	1.85	0.046
N3	LP(1)	1.86013	H4	Ry*	0.00098	1.41	2.00	0.049
O9	LP(2)	1.86596	C6-N7	σ*	0.02022	1.41	0.91	0.033
O9	LP(2)	1.86596	C10	Ry*	0.00150	1.35	1.83	0.046
C6-O9	σ	1.98928	C10-C15	σ*	0.01628	1.33	1.21	0.036
C15-C16	σ	1.97848	C19-H22	σ*	0.00539	1.33	1.03	0.033
N13	LP(1)	1.79377	H14	Ry*	0.00113	1.30	2.07	0.049
C6-N7	π	1.98553	C6-N7	π*	0.19767	1.28	0.34	0.020
N13	LP(1)	1.79377	C6	Ry*	0.00224	1.26	1.82	0.045

C10-C15	σ	1.98158	C16	Ry*	0.00252	1.23	1.45	0.038
N13-H14	σ	1.97224	C1-O2	π*	0.26091	1.23	0.66	0.027
C6-N13	σ	1.97876	C1	Ry*	0.01544	1.19	1.62	0.039
O9	LP(1)	1.96740	C10	Ry*	0.00250	1.19	1.42	0.037
N7	LP(1)	1.89597	H8	Ry*	0.00119	1.18	2.19	0.047
O9-C10	σ	1.98385	C6	Ry*	0.01543	1.15	1.69	0.039
C1-O2	π	1.99083	C1-O2	π*	0.26091	1.14	0.35	0.019
C15-C16	σ	1.97848	C19	Ry*	0.00235	1.14	1.34	0.035
O9	LP(1)	1.96740	C10-H11	σ*	0.02730	1.11	1.00	0.030
C16-C19	σ	1.98729	C15	Ry*	0.00285	1.10	1.34	0.034
C6-N13	σ	1.97876	O9-C10	σ*	0.02071	1.09	1.05	0.030
C10-H11	σ	1.98653	N7-H8	σ*	0.01276	1.08	1.03	0.030
O2	LP(2)	1.84627	C1	Ry*	0.00324	1.08	1.74	0.040
C1-N3	σ	1.99276	C6-N13	σ*	0.05443	1.07	1.07	0.031
N13-H14	σ	1.97224	C1	Ry*	0.00324	1.03	2.16	0.042
N3-H5	σ	1.98385	C1	Ry*	0.00324	1.02	2.16	0.042
O2	LP(2)	1.84627	N7	Ry*	0.00310	1.02	1.13	0.032
O9	LP(1)	1.96740	C10-C15	σ*	0.01628	1.00	0.96	0.028
O9-C10	σ	1.98385	C15-C16	σ*	0.01083	0.98	1.21	0.031
N13	LP(1)	1.79377	C1	Ry*	0.00196	0.94	1.59	0.036
N3	LP(1)	1.86013	C1	Ry*	0.00478	0.92	2.14	0.041
O9	LP(1)	1.96740	C6-N7	π*	0.19767	0.88	0.61	0.022
C6-N7	π	1.98553	N13-H14	σ*	0.01148	0.87	0.73	0.022
N13-H14	σ	1.97224	C6	Ry*	0.00176	0.87	1.84	0.036
O2	LP(1)	1.97900	C1	Ry*	0.00001	0.85	4.69	0.057
O9	LP(1)	1.96740	C6	Ry*	0.00352	0.83	2.03	0.038
N3-H5	σ	1.98385	C1-O2	π*	0.26091	0.82	0.66	0.022
N3-H4	σ	1.98434	C1-O2	π*	0.26091	0.81	0.66	0.022
O9-C10	σ	1.98385	C6-N7	π*	0.19767	0.78	0.84	0.024
C15-C16	σ	1.97848	C10	Ry*	0.00250	0.77	1.42	0.030
N13	LP(2)	1.79377	C1	Ry*	0.00478	0.77	2.15	0.038
C6-N13	σ	1.97876	C6-N7	σ*	0.02022	0.76	1.35	0.029
O2	LP(2)	1.84627	C1	Ry*	0.00001	0.75	0.98	0.025
O2	LP(2)	1.84627	N7-H8	σ*	0.01276	0.75	0.73	0.022
N7	LP(1)	1.89597	C6	Ry*	0.00461	0.75	2.27	0.03
C6-O9	σ	1.98928	C1-N13	σ*	0.08624	0.74	1.13	0.026
C6-N7	σ	1.99420	C6	Ry*	0.01543	0.72	1.75	0.032
N13	LP(1)	1.79377	C6-N7	σ*	0.02022	0.72	0.95	0.024
C6-O9	σ	1.98928	C10	Ry*	0.00250	0.70	1.66	0.030
N3	LP(1)	1.86013	C1	Ry*	0.00196	0.70	1.58	0.031
O9	LP(1)	1.96740	C6	Ry*	0.00352	0.70	2.29	0.036
C1-N13	σ	1.98146	N3-H4	σ*	0.00370	0.69	1.20	0.026
C6-N7	σ	1.99420	N13-H14	σ*	0.01148	0.69	1.29	0.027
C16-C19	σ	1.98729	C15-C16	σ*	0.01083	0.68	0.97	0.023
C1-N13	σ	1.98146	C6	Ry*	0.01543	0.66	1.63	0.029
C1-O2	π	1.99083	N13-H14	σ*	0.01148	0.65	0.76	0.020
N3-H4	σ	1.98434	C1	Ry*	0.00104	0.65	1.82	0.031
C10-C15	σ	1.98158	O9	Ry*	0.00298	0.65	1.39	0.027
C1-O2	σ	1.99539	N3-H5	σ*	0.00735	0.61	1.42	0.026
C6-N7	σ	1.99420	H8	Ry*	0.00028	0.61	3.17	0.039
C10-C15	σ	1.98158	O9	Ry*	0.00272	0.61	1.40	0.026
C1-O2	σ	1.99539	N13-H14	σ*	0.01148	0.59	1.40	0.026
C1-N13	σ	1.98146	C6-N7	π*	0.19767	0.58	0.78	0.020
N7-H8	σ	1.96628	C6	Ry*	0.00461	0.57	2.56	0.034
C10-C15	σ	1.98158	C10-H11	σ*	0.02730	0.54	1.02	0.021
C16-C19	σ	1.98729	C19-H22	σ*	0.00539	0.52	1.03	0.021
C15-C16	σ	1.97848	C16-C19	σ*	0.00613	0.51	0.97	0.020
C15-H17	σ	1.98137	C10	Ry*	0.00120	0.51	1.52	0.025
C16-C19	σ	1.98729	C16-H20	σ*	0.01453	0.51	1.02	0.020
C16-C19	σ	1.98729	C16-H21	σ*	0.01455	0.51	1.02	0.020
C1-N13	σ	1.98146	O2	Ry*	0.00342	0.50	1.52	0.025

TABLE-6
OCCUPANCY OF NATURAL ORBITALS (NBOs) AND HYBRIDS OF AB^{n}UH
CALCULATED BY B3LYP METHOD WITH 6-311G++ (d,p) BASIS SET

NBO	Occupancy	Hybridization	AO (%)
σC1-O2	1.99539	$sp^{1.91}$ (C1)	s(34.28%)p(65.56%)d(0.16%)
σC1-N3	1.99276	$sp^{2.02}$(C1)	s(33.10%)p(66.78%)d(0.12%)
σC1-N13	1.98146	$sp^{2.07}$(C1)	s(32.52%)p(67.34%)d(0.13%)
σN3-H5	1.98385	$sp^{3.19}$(N3)	s(23.87%)p(76.04%)d(0.08%)
σC6-N7	1.99420	$sp^{1.59}$(C6)	s(38.55%)p(61.37%)d(0.08%)
σC6-O9	1.98928	$sp^{2.47}$(C6)	s(28.73%)p(71.02%)d(0.25%)
σC6-N13	1.97876	$sp^{2.09}$(C6)	s(32.32%)p(67.56%)d(0.12%)
σN7-H8	1.96628	$sp^{2.86}$(N7)	s(25.87%)p(74.04%)d(0.09%)
σO9-C10	1.98385	$sp^{2.40}$(O9)	s(29.42%)p(70.52%)d(0.06%)
σC10-H11	1.98653	$sp^{2.96}$(C10)	s(25.23%)p(74.70%)d(0.08%)
σC10-C15	1.98158	$sp^{2.41}$(C10)	s(29.35%)p(70.61%)d(0.04%)
σN13-H14	1.97224	$sp^{3.59}$(N13)	s(21.79%)p(78.13%)d(0.09%)
σC15-C16	1.97848	$sp^{2.67}$(C15)	s(27.21%)p(72.76%)d(0.04%)
σC15-H17	1.98137	$sp^{3.25}$(C15)	s(23.52%)p(76.41%)d(0.07%)
σC16-C19	1.98729	$sp^{2.71}$(C16)	s(26.94%)p(73.02%)d(0.04%)
σC16-H20	1.98253	$sp^{3.31}$(C16)	s(23.18%)p(76.75%)d(0.07%)
σC16-O21	1.98253	$sp^{3.31}$(C16)	s(23.18%)p(76.75%)d(0.07%)
σC19-H22	1.98996	$sp^{3.17}$(C19)	s(23.98%)p(75.96%)d(0.06%)
πC1-O2	1.99083	$sp^{99.99}d^{7.55}$(C1)	s(0.05%)p(99.55%)d(0.40%)
πC6-N7	1.98553	$sp^{99.99}d^{0.53}$(C6)	s(0.37%)p(99.43%)d(0.20%)
lp(1)O2	1.97900	$sp^{0.56}$(O2)	s(64.20%)p(35.79%)d(0.01%)
lp(1)N3	1.89597	$sp^{3.91}$(N3)	s(20.36%)p(79.58%)d(0.05%)
lp(1)N7	1.89597	$sp^{1.96}$(N7)	s(33.74%)p(66.16%)d(0.09%)
lp(1)O9	1.96740	$sp^{1.32}$(O9)	s(43.06%)p(56.92%)d(0.03%)
lp(1)N13	1.79377	$sp^{3.61}$(N13)	s(21.69%)p(78.24%)d(0.07%)
lp(2)O2	1.84627	$sp^{99.99}d^{1.55}$(O2)	s(0.05%)p(99.88%)d(0.07%)
lp(2)O9	1.86596	$sp^{64.03}d^{0.03}$(O9)	s(1.54%)p(98.42%)d(0.04%)
σ*C1-O2	0.01366	$sp^{1.91}$(C1)	s(34.28%)p(65.56%)d(0.16%)
σ*C1-N3	0.06310	$sp^{2.02}$(C1)	s(33.10%)p(66.78%)d(0.12%)
σ*C1-N13	0.08624	$sp^{2.07}$(C1)	s(32.52%)p(67.34%)d(0.13%)
σ*N3-H4	0.00370	$sp^{2.77}$(N3)	s(26.48%)p(73.44%)d(0.08%)
σ*C6-N7	0.02022	*sp*1.59(C6)	s(38.55%)p(61.37%)d(0.08%)
σ*C6-O9	0.08883	$sp^{2.47}$(C6)	s(28.73%)p(71.02%)d(0.25%)
σ*C6-N13	0.01276	$sp^{2.09}$(C6)	s(32.32%)p(67.56%)d(0.12%)
σ*N7-H8	0.01276	$sp^{2.86}$(N7)	s(25.87%)p(74.04%)d(0.09%)
σ*O9-C10	0.02071	*sp*2.40(O9)	s(29.42%)p(70.52%)d(0.06%)
σ*C10-H11	0.02730	$sp^{2.96}$(C10)	s(25.23%)p(74.70%)d(0.08%)
σ*C10-H12	0.02177	$sp^{2.98}$(C10)	s(25.10%)p(74.82%)d(0.08%)
σ*C10-C15	0.01628	$sp^{2.41}$(C10)	s(29.35%)p(70.61%)d(0.04%)
σ*N13-H14	0.01148	$sp^{3.59}$(N13)	s(21.79%)p(78.13%)d(0.09%)
σ*C15-C16	0.01083	$sp^{2.67}$(C15)	s(27.21%)p(72.76%)d(0.04%)
σ*C15-H17	0.01430	$sp^{3.25}$(C15)	s(23.52%)p(76.41%)d(0.07%)
σ*C16-C19	0.00613	$sp^{2.71}$(C16)	s(26.94%)p(73.02%)d(0.04%)
σ*C16-H20	0.01453	$sp^{3.31}$(C16)	s(23.18%)p(76.75%)d(0.07%)
σ*C19-H22	0.00539	$sp^{3.17}$(C19)	s(23.98%)p(75.96%)d(0.06%)

antibonding orbitals of the (AB^{n}UH) molecule are mainly contributed to *p*-type subshell.

Theoretical UV-visible spectra and solvent effect: In this study, the electronic transition between the lowest singlet → singlet spin allowed excited states are taken into account. The maximum absorption wavelengths (λ_{max}), excitation energies (ΔE) and oscillator strength (f) of the molecule (AB^{n}UH) are computed using TD-DFT/B3LYP/6-311++G (d,p) method in the gaseous state and in different solvents. The simulated UV-visible spectrum of the compound under study in gaseous state and the molecule in different solvent is presented in Fig. 5. Polarizable continuum model TD-DFT method with B3LYP/6-311++G (d,p) basis set are applied to investigate solvent effect on the absorption wavelength and excitation energy. The molecule under study have shown three maximum absorption peaks at 291.24, 260.4 and 250.71 nm due to excitation from HOMO → LUMO, HOMO+1 → LUMO and HOMO → LUMO+1, respectively. The other excitation wavelengths with their peaks in different solvents are presented in Table-7.

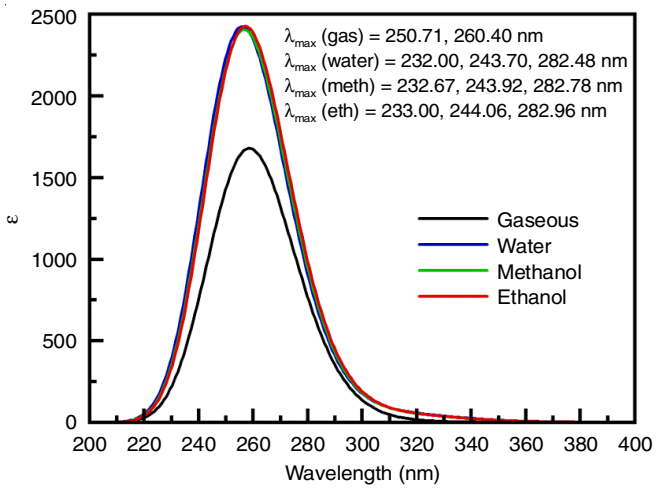

Fig. 5. Calculated UV-visible spectra of 1-amidino-*n*-butyl urea in different solvent using TD-DFT/B3LYP/6-311++G(d,p)

Vibrational analysis: The calculated theoretical frequencies and infrared intensities along with PED analysis using B3LYP/6-311++G(d,p) methods of the optimized geometry of the compound are reported in Table-8 to obtain the spectroscopic signature so as to assign the observed bands. The PED analysis is an accurate method to describe quantitative contribution of movement of a given group of atoms in a normal mode. It is indeed a fact that in this study, we did not compare for any agreement between the experimental and calculated values to find a correlation of the applied method (DFT/6-311++G(d,p). The theoretical vibrational analysis values are generally somewhat greater than the experimental values due to lack of necessary correction to be made in terms of anharmonicity or using proper factor of the real system. The optimized molecular geometry of the compound (AB^nUH) shows C1 symmetry, which implies 66 active vibrational normal modes along with 3 translational and 3 rotational motions. The assignment of the these vibrational modes has been performed at the B3LYP/6-311++ G(d,p) level. All the 66 fundamental modes of vibration are IR active. The compound (AB^nUH) has 22 stretching modes, 21 torsional modes of vibration and 23 bending modes of vibrations. In this study, empirical scaling factors were not applied to correct the effect of anharmonicity due to lack of experimental data.

TABLE-7
TRANSITION BETWEEN MOLECULAR ORBITALS CORRESPONDING WAVELENGTHS, ENERGY AND OSCILLATORY STRENGTH (*f*)

State of molecule	Transition	Wavelength (nm)	Energy (eV)	Oscillatory strength (*f*)
Gaseous	i) H → L; H → L+1; H → L+2	i) 291.24	i) 4.2572	i) 0.0004
	ii) H → L; H → L+1	ii) 260.4	ii) 4.7612	ii) 0.0339
	iii) H−3 → L+1; H → L+1; H → L+2	iii) 250.71	iii) 4.9452	iii) 0.0089
In water	i) H → L; H → L+1	i) 282.48	i) 4.3891	i) 0.0012
	ii) H → L+2; H → L+3	ii) 243.74	ii) 5.0866	ii) 0.0125
	iii) H → L; H → L+1	iii) 231.92	iii) 5.3461	iii) 0.0524
In methanol	i) H → L; H → L+1	i) 282.68	i) 4.3860	i) 0.0012
	ii) H−3 → L; H → L+2; H → L+3	ii) 243.90	ii) 5.0834	ii) 0.0125
	iii) H → L; H → L+1	iii) 232.37	iii) 5.3357	iii) 0.0520
In ethanol	i) H → L; H → L+1	i) 282.81	i) 0.0012	i) 0.0012
	ii) H−3 → L; H → L+2; H → L+3	ii) 244.01	ii) 0.0127	ii) 0.0127
	iii) H → L; H → L+1	iii) 232.63	iii) 0.0523	iii) 0.0523

TABLE-8
THEORETICAL FREQUENCIES AND INFRARED INTENSITIES ALONG WITH THE PED ANALYSIS OF AB^{n}UH CALCULATED WITH B3LYP/6-311++G METHOD

Frequency (cm^{-1})	Intensity	PED contribution (%)
28.5	491.79	76 $\tau C_1N_{13}C_6O_9$
51.1	205.45	86 $\tau C_{10}O_9C_6N_{13}$
59.2	149.41	73 $\tau C_6O_9C_{10}C_{15}$
66.4	62.30	55 $\beta_{rock}C_{15}C_{10}O_9$
101.7	110.79	55 $\tau_{as}C_6N_{13}C_1N_3$
125.4	18.46	64 $\tau C_6O_9C_{10}C_{15}$
154.2	18.62	55 $\tau C_{10}O_9C_6N_{13}$
180.9	74.07	59 $\beta_{scis}C_1N_{13}C_6$
248.8	1.24	94 $\tau H_{22}C_{19}C_{16}C_{15}$
259.1	24.94	32 νO_9C_{10} + 41 $\beta_{scis}C_{10}C_{15}C_{16}$
272.3	2.26	69 $\beta_{scis}C_{15}C_{16}C_{19}$
398.5	192.06	37 $\beta_{scis}N_3C_1N_{13}$
412.0	499.46	62 $\tau H_5N_3C_1N_{13}$
440.9	83.03	68 $\beta_{scis}C_{15}C_{16}C_{19}$
474.2	28.53	53 $\beta C_{10}C_{15}C_{16}$
491.0	1041.42	52 $\tau_{as}H_{14}N_{13}C_1N_3$
552.7	976.01	71 $\tau H_4N_3C_1N_{13}$
608.3	288.78	66 $\beta_{sci}N_7C_6O_9$
689.4	102.42	61 $\tau H_8N_7C_6N_{13}$
747.2	115.10	39 $\tau H_{11}C_{10}O_9C_6$ + 11 $\tau H_{11}C_{10}O_9C_6$
749.8	241.22	21 $\beta_{wagging}N_7C_6O_9$ + 24 $\tau H_8N_7C_6N_{13}$
759.3	437.68	64 $\tau H_8N_7C_6N_{13}$
775.2	78.36	51 $\tau_{as}H_8N_7C_6N_{13}$
825.1	27.36	59 $\tau_{as}H_{11}C_{10}O_9C_6$
902.9	7.64	48 $\nu C_{15}C_{16}$ + 19 $\tau H_{23}C_{19}C_{16}C_{15}$
948.4	40.89	46 $\nu N_{13}C_1$
961.0	0.76	31 $\tau H_{11}C_{10}O_9C_6$ + 20 $\beta H_{20}C_{16}C_{19}$ +15 $\beta H_{12}C_{10}O_9$
972.6	218.98	25 νO_9C_6 + 12 $\beta C_{10}C_{15}C_{16}$
1028.5	24.32	67 $\nu_{as}C_{10}C_{15}$
1068.4	12.03	73 $\nu_{as}C_{10}C_{15}$
1087.8	505.61	42 $\beta_{scis}H_8N_7C_6$ + 20 $\nu N_{13}C_6$ + 15 $\nu_{as}N_{13}C_1$
1096.1	1109.88	44 νN_3C_1 + 11 $\beta H_4N_3C_1$
1124.0	115.11	22 $\beta H_4N_3C_1$ + 16 νO_9C_{10} + 13 $\nu N_{13}C_6$ + 15 $\nu C_{15}C_{16}$
1144.0	14.25	21 $\tau H_{23}C_{19}C_{16}C_{15}$ + 15 β $C_{10}C_{15}C1_6$ + 13 β $C_{10}C_{15}C1_6$ +12 $\nu C_{15}C_{16}$
1187.2	6.45	51 $\tau H_{17}C_{15}C_{16}C_{19}$ + 12 $\beta H_{20}C_{16}C_{19}$
1250.4	1164.02	23 $\beta H_8N_7C_6$ + 18 $\beta_{rock}H_{14}N_{13}C_1$ + 12 $\beta H_4N_3C_1$ +
1253.8	77.42	59 β_{scis} $H_{12}N_{10}O_9$
1299.1	28.75	49 $\tau H_{11}C_{10}O_9C_6$
1320.4	0.28	57 β_{scis} $H_{20}C_{16}C_{19}$ + 14 $\tau H_{11}C_{10}O_9C_6$
1326.4	348.70	24 β_{scis} $H_4N_3C_1$ + 12 νN_3C_1 + 11 β $H_8N_7C_6$
1329.8	2.46	78 β_{twi} $H_{17}C_{15}C_{16}$
1387.9	2.33	48 $\tau H_{11}C_{10}O_9C_6$
1413.4	17.84	87 $\beta_{rock}H_{22}C_{19}H_{23}$
1422.9	63.06	58 $\tau H_{11}C_{10}O_9C_6$
1491.9	2.00	73 β_{scis} $H_{20}C_{16}N_{21}$
1497.7	1.00	63 β_{scis} $H_{17}C_{15}H_{18}$ + 13 $\tau H_{23}C_{19}C_{16}C_{15}$
1501.0	22.89	77 $\beta_{twi}H_{22}C_{19}H_{23}$
1509.6	71.93	69 β_{scis} $H_{11}C_{10}H_{12}$
1521.14	357.17	66 β_{scis} $H_{23}C_{19}H_{24}$
1537.6	1447.23	44 β_{scis} $H_{14}N_{13}C_1$ + 13 $\nu N_{13}C_6$ + 11 β_{scis} $H_{23}C_{19}H_{24}$
1628.2	191.01	81 β_{scis} $H_5N_3H_4$
1727.6	289.06	69 νN_7C_6
1826.8	1048.49	70 νO_2C_1
3003.2	7.48	83 $\nu_sC_{10}H_{11}$ + 16 $\nu C_{16}H_{20}$
3009.2	35.29	77 $\nu_sC_{16}H_{20}$ + 13 $\nu C_{10}H_{11}$
3021.8	28.06	86 $\nu_sC_{19}H_{22}$
3028.5	65.92	78 $\nu_sC_{15}H_{17}$
3031.5	12.02	75 $\nu_sC_{16}H_{20}$ + 13 $\nu C_{15}H_{17}$
3041.1	5.90	79 $\nu_{as}C_{10}H_{11}$ + 13 $\nu_{as}C_{15}H_{17}$
3071.9	27.03	61 $\nu_sC_{15}H_{17}$ + 18 $\nu_{as}C_{19}H_{23}$ + 17 $\nu_{as}C_{10}H_{11}$
3085.6	102.49	76 $\nu_{as}C_{19}H_{23}$ +11$\nu_{as}C_{15}H_{17}$ + 11$\nu C_{16}H_{20}$
3090.4	48.61	94 $\nu_{as}C_{19}H_{22}$
3557.6	10.31	100 νN_7H_8
3571.0	39.05	99 $\nu_sN_3H_4$
3624.1	43.29	99 $\nu_{as}N_{13}H_{14}$
3683.2	40.83	99 $\nu_{as}N_3H_4$

N-H vibration: N-H stretching of AB^{n}UH is calculated to observe at 3683-3557 cm^{-1} with PED contribution 99-100%. Of the four N-H stretching vibrations two are observed to contribute from symmetric and other two due to asymmetric stretching as calculated by VEDA 4 program.

C-H vibration: According to the PED analysis all the C-H stretching modes are assigned between the frequencies ranges from 3090-3003 cm^{-1} at different intensities with PED contribution 61-94% without mixed vibrations. The maximum PED contribution of the vibrational modes are from symmetric stretching with low intensity while the antisymmetric stretching of C-H bond at 3041 cm^{-1} (79% PED contribution), 3085 cm^{-1} (with 102.49 intensity and 76% PED contribution) and at 3090 cm^{-1} with 94% PED and 48.61 intensity were observed. The C-H bending (scissoring) are expected to occur from 1470-1450 cm^{-1} however in the present study C-H scissoring occur around 1553-1491 cm^{-1} with varied intensity ranges from 1-357 and PED contribution 63-77%. The rocking mode of the vibration is exhibited at 1413 with intensity 17 from 87% contribution of PED.

Carbonyl (C=O) vibration: The vibration around 1850-1550 cm^{-1} corresponds to strong C=O stretching of the carbonyl group [23]. The functional group such as ester, ketone or amide group are identified with a differences of 20-30 cm^{-1} in the vibration. In the present study, the stretching mode due to C=O is predicted at 1826.8 cm^{-1} due to amide group.

Conclusion

The present study is an attempt to explore the ground state geometries, spectral (IR and UV-vis) properties, natural bond orbital (NBO) analysis, electrostatic potentials and frontier orbital analysis of 1-amidino-O-(*n*-butyl)urea (AB^{n}UH) by density functional B3LYP and TD-DFT methods using standard 6-311++G (d,p) basis set. The energy band gap is calculated by using HOMO and LUMO analysis. The NBO analysis have discussed about the accumulation of electrons in core, valence and Rydberg sub-shell of their atomic orbitals, the subshell type, the contribution of specified atomic electrons to s-type and p-type sub-shells and their hybridization. Electrostatic surface analysis showed the highest electron density on the atom N3 with -0.82353e indicating the site for electrophilic

attack while the maximum positive region on C1 with 0.79583e thereby showing the possible site for nucleophilic attack. The second order perturbation results have shown that the most significant hyperconjugative interactions is observed in the non-bonding interaction between O2 (lp) and antibonding C1-N13 followed by interaction between N3 (lp) and C1-O2 (s*), O2 (lp) and C1-N3, respectively. The maximum absorption wavelength due to electronic transition, vertical excitation energies and oscillator strengths are found out by PCM of TD-DFT/B3LYP/6-311++G(d,p) method and shown the allowed and forbidden transition along with the solvent effect. The assignment of the calculated fundamental vibrational modes of the titled compound was performed on the basis of potential energy distribution (PED) analysis by using VEDA 4.0 program and the structure of 1-amidino-O-(*n*-butyl) urea using VEDA 4.0 Program is assigned in Fig. 6.

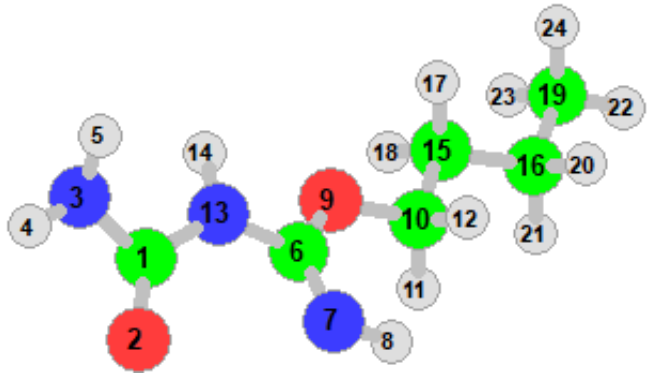

Fig. 6. Structure of 1-amidino-O-(*n*-butyl) urea using VEDA 4.0 program

CONFLICT OF INTEREST

The authors declare that there is no conflict of interests regarding the publication of this article.

REFERENCES

1. F.M. Moghaddam, M. Daneshfar, Z. Daneshfar, A. Iraji, A. Samandari-Najafabad, M.A. Faramarzi and M. Mahdavi, *J. Mol. Struct.*, **1250**, 131726 (2022); https://doi.org/10.1016/j.molstruc.2021.131726
2. S.P. Devi, L.J. Singh, N.S. Devi, R.K. Bindiya Devi and R.K. Hemakumar Singh, *J. Coord. Chem.*, **70**, 2492 (2017); https://doi.org/10.1080/00958972.2017.1344232
3. L.J. Singh, N.S. Devi, S.P. Devi, W.B. Devi, R.K.H. Singh, B. Rajeswari and R.M. Kadam, *Inorg. Chem. Commun.*, **13**, 365 (2010); https://doi.org/10.1016/j.inoche.2009.12.023
4. N.S. Devi, L.J. Singh, S.P. Devi, R.K.B. Singh, R.K.H. Singh, B. Rajeswari and R.M. Kadam, *J. Coord. Chem.*, **64**, 4108 (2011); https://doi.org/10.1080/00958972.2011.635789
5. T.C. Zeyrek, *J Korean Chem. Soc.*, **57**, 461 (2013); https://doi.org/10.5012/jkcs.2013.57.4.461
6. S. Muthu, N.R. Sheela and S.S. Krishnan, *Mol. Simul.*, **37**, 1276 (2011); https://doi.org/10.1080/08927022.2011.597395
7. P.K. Chattaraj, B. Maiti and U. Sarkar, *J. Phys. Chem. A*, **107**, 4973 (2003); https://doi.org/10.1021/jp034707u
8. V. Vidhya, A. Austine and M. Arivazhagan, *Heliyon*, **5**, e02365 (2019); https://doi.org/10.1016/j.heliyon.2019.e02365
9. V. Balachandra, T. Karthick, S. Perumal and A. Nataraj, *Indian J. Pure Appl. Phys.*, **51**, 178 (2013).
10. I. Sidir, Y.G. Sidir, M. Kumalar and E. Tasal, *J. Mol. Struct.*, **964**, 134 (2010); https://doi.org/10.1016/j.molstruc.2009.11.023
11. Z.B. Maksic, Molecular Spectroscopy, Electronic Structure and Intramolecular Interactions. Springer-Verlag Berlin Heidelberg GmbH, New York (1991).
12. S. Fliszár, Charge Distributions and Chemical Effects, Charge Distributions and Chemical Effects, Springer-Verlag: Berlin Heidelberg GmbH, Tokyo (1983).
13. H. Pir, N. Günay, D. Avci and Y. Atalay, *Spectrochim. Acta A Mol. Biomol. Spectrosc.*, **96**, 916 (2012); https://doi.org/10.1016/j.saa.2012.07.044
14. G. Gece, *Corros. Sci.*, **50**, 2981 (2008); https://doi.org/10.1016/j.corsci.2008.08.043
15. I. Fleming, Molecular Orbitals and Organic Chemical Reactions, A John Wiley & Sons, Ltd., pp 1–515 (2010).
16. L.R. Domingo, M.J. Aurell, P. Pérez and R. Contreras, *Tetrahedron*, **58**, 4417 (2002); https://doi.org/10.1016/S0040-4020(02)00410-6
17. A.E. Reed, R.B. Weinstock and F. Weinhold, *J. Chem. Phys.*, **83**, 735 (1985); https://doi.org/10.1063/1.449486
18. A. Ali, M. Khalid, M.A. Rehman, F. Anwar, H. Zain-Ul-Aabidin, M.N. Akhtar, M.U. Khan, A.A.C. Braga, M.A. Assiri and M. Imran, *ACS Omega*, **5**, 18907 (2020); https://doi.org/10.1021/acsomega.0c02128
19. N.R. Sheela, S. Muthu and S. Sampathkrishnan, *Spectrochim. Acta A Mol. Biomol. Spectrosc.*, **120**, 237 (2014); https://doi.org/10.1016/j.saa.2013.10.007
20. W. Kiefer, *J. Raman Spectrosc.*, **38**, 1538 (2007); https://doi.org/10.1002/jrs.1902
21. J.N. Liu, Z.R. Chen and S.F. Yuan, *J. Zhejiang Univ. Sci.*, **6B**, 584 (2005); https://doi.org/10.1631/jzus.2005.B0584
22. M. Snehalatha, C. Ravikumar, I.H. Joe, N. Sekar and V.S. Jayakumar, *Spectrochim. Acta A Mol. Biomol. Spectrosc.*, **72**, 654 (2009); https://doi.org/10.1016/j.saa.2008.11.017
23. G. Socrates, Infrared and Raman Characteristic Group Frequencies. Tables and Charts, John Wiley & Sons Ltd., Edn. 3 (2004).